Statistical Estimation of the Efficiency of Quantum State Tomography Protocols

Yu. I. Bogdanov,[1] G. Brida,[2] M. Genovese,[2] S. P. Kulik,[3] E. V. Moreva,[4,5] and A. P. Shurupov[2,6]

[1]*Institute of Physics and Technology, Russian Academy of Sciences, 117218, Moscow, Russia*
[2]*INRIM, I-10135, Torino, Italy*
[3]*Faculty of Physics, Moscow State University, 119992, Moscow, Russia*
[4]*Moscow National Research Nuclear University "MEPHI", 115409, Moscow, Russia*
[5]*International Laser Center of M.V. Lomonosov, Moscow State University, 119991, Moscow, Russia*
[6]*Dipartimento di Fisica, Politecnico di Torino, I-10129, Torino, Italy*

(Received 18 February 2010; published 1 July 2010)

A novel operational method for estimating the efficiency of quantum state tomography protocols is suggested. It is based on *a priori* estimation of the quality of an arbitrary protocol by means of universal asymptotic fidelity distribution and condition number, which takes minimal value for better protocol. We prove the adequacy of the method both with numerical modeling and through the experimental realization of several practically important protocols of quantum state tomography.

DOI: 10.1103/PhysRevLett.105.010404 PACS numbers: 03.65.Wj, 03.67.Bg, 42.50.Dv

Introduction.—Quantum states and processes being a fundamental tool for basic research, also become a resource for developing quantum technologies [1,2]: this demands for their characterization. At present quantum state or process tomography serves as a standard instrument [2–12] for characterizing quality of preparation and transformation of quantum states. Basically, it includes a given set of unitary transformations over the state to be reconstructed, then the transformed state is measured, and finally some computational procedure applied to the measuring outcomes completes the state reconstruction. The result is a state vector or a density matrix.

It is worth mentioning that in real experiments the accuracy of the reconstruction depends on two types of uncertainties: statistical and instrumental ones. If the total number of measurement outcomes (sample size or statistics) is large enough, the instrumental uncertainties dominate over fundamental statistical fluctuations caused by the probabilistic nature of quantum phenomena [4]. Practically, the required statistics, allowing to exclude statistical fluctuations, depends on the tomographic protocol itself and the total accumulating time needed for taking data. From this point of view it is of the utmost interest to point out simple and universal algorithms for the estimation of the chosen protocol on the design stage before doing experiments, as well as the sample size for desirable quality of the state reconstruction.

In order to provide a useful tool for choosing a tomographic scheme optimal for a given setup, in this Letter we propose a universal method for estimating the quality of any tomographic protocol based on discrete degrees of freedom and we test it with well-known reconstruction protocols of polarization states of qubit pairs. Since it represents a paradigmatic example, here we consider polarization degrees of freedom only.

Theory and numerical simulation.—An arbitrary s-dimensional quantum state is completely described by a state vector in a s-dimensional Hilbert space when it is a pure state, or by a density matrix ρ for a mixed one. To measure the quantum state one needs to perform a set of projective measurements on a set of identical states.

In general an arbitrary protocol based on m measurements can be compactly written in the matrix form [2,13]:

$$T = B\rho, \tag{1}$$

where ρ is the density matrix, given in the form of a column (second column lies below the first, etc.) and B is the measurement matrix ($m \times s^2$). The vector T of length m records the total number of registered outcomes. The algorithm that we use for solving Eq. (1) is based on the so called singular value decomposition (svd) [14]. Svd serves as a base for solving inverse problem by means of pseudoinverse (PI) or Moore-Penrose inverse [15]. In summary, the matrix B can be decomposed as

$$B = USV^{+}, \tag{2}$$

where U ($m \times m$) and V ($s^2 \times s^2$) are unitary matrices and S ($m \times s^2$) is a diagonal, non-negative matrix, whose diagonal elements are "singular values". Then (1) transforms to a simple diagonal form

$$Sf = Q \tag{3}$$

with a new variable f unitary related to ρ as $f = V^{+}\rho$ and a new column Q unitary related to the vector T as $Q = U^{+}T$. We use this algorithm as a starting approximation for maximal likelihood state reconstruction. By defining q as the number of nonzero singular values of B we formulate two important conditions of any tomography protocol, namely, its completeness and adequacy. The protocol is supposed to be informationally complete if the number of tomographically complementary projection measurements is equal to the number of parameters to be estimated; mathematically completeness means $q = s^2$. Adequacy

means that the statistical data directly correspond to the physical density matrix (which has to be normalized, Hermitian and positive). However, generally for mixed state it can be tested only if the protocol consists of redundant measurements, i.e., $m > q$.

As mentioned, PI provides with zero approximation for estimated parameters of quantum states. Optimization of these parameters can be done following the approach developed in [4] in the frame of maximal likelihood method. It is worth to stress that the reconstructed state vector extracted from the likelihood equation associates with finite statistics of the registered outcomes of an experiment and therefore takes random values. The difference between the reconstructed state vector and its exact value is caused by statistical fluctuations [16]. The complete information matrix introduced in [4,13] allows analyzing arbitrary functions on fluctuating parameters of quantum states. One very relevant function in the context of quantum state/process estimation is fidelity $F = [\mathrm{Tr}\sqrt{\sqrt{\rho_0}\rho\sqrt{\rho_0}}]^2$, where ρ_0 and ρ being the exact and the reconstructed density matrices correspondingly, tending to identity for complete protocols with an unlimited increase of the sample size.

Basically the problem of the state reconstruction splits into two scenarios. The first one relates to the case when the reconstructed state is known in advance (like in quantum cryptography). Then statistical comparison between exact theoretical state and reconstructed one allows one either to reveal the source of instrumental uncertainties or to be sure that such uncertainties are small enough in comparison with statistical fluctuations. The second case occurs when the reconstructed state is unknown. Then using the approach developed below one should calculate the statistical distribution of fidelity between unknown exact state and reconstructed (by means of maximal likelihood method) one. Fidelity will be either inside the uncertainty boundary for small statistics or outside for large statistics (when instrumental uncertainties prevail). In this case it is convenient to analyze the so called fidelity loss $dF = 1 - F$. When the reconstruction accuracy is determined by a finite number of representatives of the quantum state, fidelity loss is a random variable whose asymptotic distribution can be represented as [17]

$$1 - F = \sum_{j=1}^{j_{\max}} d_j \xi_j^2, \tag{4}$$

where $\xi_j \sim N(0, 1)$ are independent and normally distributed random variables with zero mean values and unit variance, $d_j \sim \frac{1}{n} > 0$, $j_{\max} = 2s - 2$ for pure states, $j_{\max} = s^2 - 1$ for mixed states. The coefficients d_j can be extracted from the complete information matrix [17]. Distribution (4) is a natural generalization of the χ^2—distribution for which all $d_j = 1$. As it follows from (4) the average value of fidelity loss is

$$\langle 1 - F \rangle = \sum_{j=1}^{j_{\max}} d_j \tag{5}$$

PI implies introduction of so called condition number K, which is defined as the ratio between the minimal nonzero singular eigenvalue of B and maximal one

$$K = \frac{b_{\max}}{b_{\min}}. \tag{6}$$

K determines the stability of the linear system (1) and therefore can be used as a practical quantifier for estimating efficiency of the protocol: the lower K the better the protocol. If at least one of s^2 singular eigenvalues b_j is close to zero then the protocol becomes incomplete and $K \to \infty$. The optimal value of K would be unity that means uniform distribution of singular values.

The present approach allows to analyze arbitrary protocols of statistical reconstruction of quantum states. As an example we have selected three popular protocols. The first, suggested in [5] and dubbed J16 [10], is suited for reconstructing four-dimensional polarization states, as photon pairs degenerate in frequency generated in the process of spontaneous parametric down-conversion (SPDC). In this protocol the projective measurements upon some components of Stokes vector are performed for each qubit in pair individually, so the 16 two-qubit measurements are HH, HV, VV, VH, RH, RV, DV, DH, DR, DD, RD, HD, VD, VL, HL, RL, where H, V, R, L, D denotes horizontal, vertical, right and left circular and 45° diagonal polarizations, respectively. Here, for example, the measurement setting HR means measuring horizontal polarization on the first qubit and right circular polarization on the second qubit in pair. In our formalism the protocol can be represented by an instrumental matrix with 16 rows.

In the case of independent measurement of two qubits the projective measurements can be chosen arbitrarily. In [8] measured qubits were projected on the states possessing tetrahedral symmetry (protocol R16). There are several works showing that due to the high symmetry such proto-

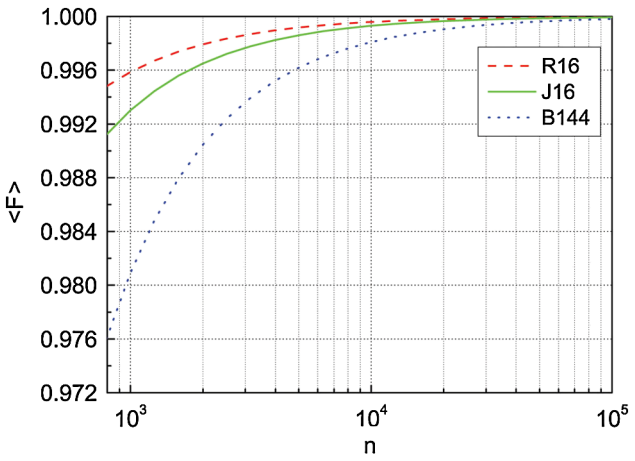

FIG. 1 (color online). Dependence of the average fidelity on number of registered events forming the sample.

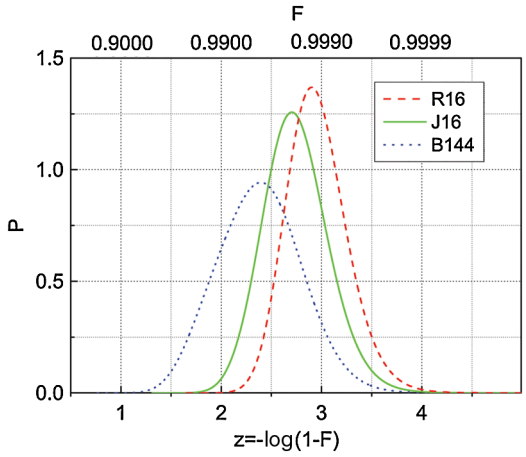

FIG. 2 (color online). Density distribution of the scaled fidelity z (lower abscissa) at $n = 3 \times 10^3$. Upper abscissa presents regular fidelity.

col provides a better quality of reconstruction [9,10]. Let us stress that since $m = s^2 = 16$ the adequacy of both R16 and J16 protocols cannot be tested.

We also consider a protocol where the whole single-beam two-qubit state is subjected to linear transformations using two retardation plates [6] (protocol B144). The total number of projective measurements is redundant and equals to 144, so the corresponding instrumental matrix has 144 rows and protocol admits adequacy testing, being $m > 16$. For these protocols we calculate condition numbers K which take the following values: $K_{\mathrm{R16}} = 3$, $K_{\mathrm{J16}} \approx 10$, $K_{\mathrm{B144}} \approx 60$ (Condition number for protocol B144 can be optimized by choosing appropriate plates). Thus, we expect that the symmetrical protocol R16 provides with better state reconstruction quality [10]. We have checked this statement with numerical simulations of each protocol applied to different two-qubit states depending on the sample size.

As an example, let us consider the numerical reconstruction of the Bell state $|\Phi^-\rangle = \frac{1}{\sqrt{2}}(|H_1H_2\rangle - |V_1V_2\rangle)$. Figure 1 shows average fidelities, calculated according to (5) as functions of sample size for each protocol. It turns out that the difference between curves disappears at sufficiently large sample size (10^5) [16], but for the same quality of state reconstruction the correct choice of protocol allows using a smaller set of statistical data; i.e., finally reduces total acquisition time. Figure 1 shows that protocols are ranged in accuracy as following: R16, J16, and B144 in complete agreement with the range given by condition number K. Figure 2 presents accuracy distributions calculated according to (4) for the sample size 3×10^3. For better visualization we transformed the abscissa scale into particular common logarithmic one as $z = -\log(1 - F)$. Corresponding integers indicate the number of nines in fidelity recording. The density distribution for the R16 protocol is narrower than that for protocols J16 and B144 and localizes in the region of lower losses or higher fidelities. The distribution for protocol B144 is broader and lower in comparison with protocols R16 and J16. Obviously, the narrower distribution of fidelity indicates a better reconstruction quality in the sense that the reconstruction procedure returns a better-defined state. Thus, Fig. 2 confirms our expectation based on estimation of condition number K: Protocol R16 achieves the best results.

Experiment.—We prepared a family of two-photon polarization states which can be easily converted into both entangled (in polarization) and factorized states

$$|\Psi\rangle = (c_1|H_1H_2\rangle + c_2 e^{i\varphi}|V_1V_2\rangle) \tag{7}$$

with real amplitudes c_1 and c_2. The setup is schematically depicted in Fig. 3. A cw argon laser beam at $\lambda = 351$ nm pumps, after having selected by a Glan-Thompson prism (GP) its horizontal polarization, two type-I BBO crystals (1 mm) positioned with the planes that contain optical axes orthogonal to each other. The half-wave plate placed in front of crystals ($\lambda_p/2$) rotates the polarization of the pump by the angle ϕ which controls real amplitudes c_1 and c_2 in (7). The crystals are cut for collinear frequency nondegenerate phase matching around central wavelength 702 nm. The relative phase shift φ in (7) is controlled by tilting quartz plates QP. If $\phi = 0$ we prepare the state $|\Psi\rangle = |V_1V_2\rangle$, if $\phi = 22.5$ and $\varphi = 3\pi/2$ then the state transforms to $|\Psi\rangle = \frac{1}{\sqrt{2}}(|H_1H_2\rangle - |V_1V_2\rangle) \equiv |\Phi^-\rangle$.

To maintain stable phase-matching conditions, BBO crystals and QP are placed in a closed box heated at fixed temperature. The lens L couples SPDC light into the monochromator M (with 1 nm resolution), set to transmit "idler" photons at 710 nm. The conjugate "signal" wavelength 694 nm is selected automatically by means of coincidence scheme. Zero-order wave plates ($\lambda/2$, $\lambda/4$) are used in both protocols J16 and R16 for arranging the

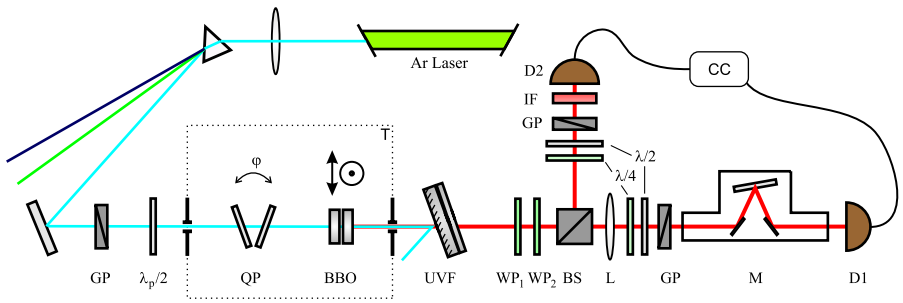

FIG. 3 (color online). Experimental setup for different tomographic reconstructions of photon pairs with variable polarization entanglement.

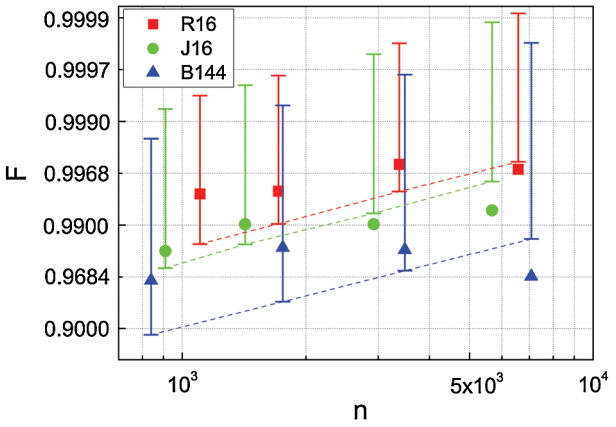

FIG. 4 (color online). Reconstruction of $|\Phi^-\rangle$ state in function of the sample size n. Vertical bars show 1%- and 99%—quantiles for fidelity distributions. Dotted lines, connecting lower bar ends, indicate critical significant levels. The experimental data, with no uncertinty bars, pertaining the specific state $|\Phi^-\rangle$ are denoted by squares, circles and triangles for R16, J16 and B144 protocols, respectively.

projective measurement set. In protocol B144 these plates were removed and additional achromatic quartz plates $WP_{1,2}$ (0.9183 mm, 0.9167 mm) established the necessary measurement set at given wavelengths [6].

For protocols described above the statistical reconstruction of prepared states (7) has been performed at given sample sizes. Our results are summarized in Fig. 4 in function of the sample size n. Here we present the calculated theoretical widths of fidelity distributions at 1%- and 99%- quantiles (vertical bars) for the three protocols (see Fig. 2), as well as the experimentally reconstructed values for the specific state $|\Phi^-\rangle$ (squares, circles and triangles for R16, J16 and B144 protocols, respectively).

First of all we note that the bar for B144 protocol exceeds corresponding bar of protocol R16 by a factor of 10 at fixed sample size, which clearly indicates better quality of protocol R16 [notice log scale in the ordinate axis]. The approach described above provides the ideal accuracy level for quantum state reconstruction. It means that fluctuations of the estimated quantum states certainly cannot lead to uncertainties smaller than this limit (i.e., at 1% confidence level the data should fall inside vertical bars in Fig. 4). Nevertheless, the presence of instrumental uncertainties can lead to exceed this level. Indeed, Fig. 4 shows that, above some specific sample size, the experimental value of fidelity falls out the theoretical uncertainty boundary shown as dotted lines (corresponding to 1% significance level which characterizes a given protocol). This happens since instrumental uncertainties prevail over the statistical ones and indicates that either state preparation stage or measurement procedure were not performed accurately enough. Practically it means that it is meaningless to increase number of measurements further but improving of experimental procedure is really needed instead. Incidentally, the absence of uncertainty bars for data in Fig. 4 derives from running once the corresponding protocol. Figure 4 relates to a single measurement and aims to verify agreement between experimental data and the theoretical distribution in (6). For repeated measurements and associated statistical uncertainty, we shall substitute distribution of random variable F with distribution of its sample mean $\langle F\rangle$ in order to describe theoretical uncertainty.

Definitely comparison between reconstructed states and fundamental statistical fluctuations can serve to achieve precise adjustment of the setup, detection of the unapproved incursion into communication channel, etc.

Conclusion.—We have proposed and tested, both by numerical calculation and experimental realization, a new estimation scenario of tomographic protocols. Our results demonstrate the potentialities of this method for a widespread application to experiments on fundamental quantum optics and quantum technologies. Indeed, it can provide in advance, based on condition number K, indications on the uncertainty that can be reached for a certain setup by a tomographic scheme, providing experimentalist with a tool for choosing the best protocol based on available experimental resources (retardant plates, polarization filters, etc.) and limited available time for data acquisition. Also we would like to stress that the developed method is quite general and that it can be applied to any sort of quantum states and measurement sets.

This work was supported in part by Russian Foundation of Basic Research (projects 08-02-00741a, 10-02-00204a, 08-07-00481a, 10-02-00414-a), MIUR (PRIN 2007FYETBY) and NATO (CBP.NR.NRCL.983251).

[1] M. Genovese, Phys. Rep. **413**, 319 (2005).
[2] A. Ibort *et al.*, Phys. Scr. **79**, 065013 (2009).
[3] A. I. Lvovsky *et al.*, Phys. Rev. Lett. **87**, 050402 (2001); A. Zavatta, S. Viciani, and M. Bellini, Phys. Rev. A **70**, 053821 (2004); A. Allevi *et al.*, Phys. Rev. A **80**, 022114 (2009); G. Zambra *et al.*, Phys. Rev. Lett. **95**, 063602 (2005).
[4] Yu. Bogdanov *et al.*, Phys. Rev. A **70**, 042303 (2004).
[5] D. F. V. James *et al.*, Phys. Rev. A **64**, 052312 (2001).
[6] Yu. Bogdanov *et al.*, Phys. Rev. A **73**, 063810 (2006).
[7] G. M. DAriano, P. Mataloni, and M. F. Sacchi, Phys. Rev. A **71**, 062337 (2005).
[8] J. Rehacek, B.-G. Englert, and D. Kaszlikowski, Phys. Rev. A **70**, 052321 (2004).
[9] A. Ling *et al.*, Phys. Rev. A **74**, 022309 (2006); A. Ling *et al.*, arXiv:0807.0991.
[10] N. D. de Burgh *et al.*, Phys. Rev. A **78**, 052122 (2008).
[11] M. Asorey *et al.*, Phys. Rev. A **77**, 042115 (2008).
[12] G. Brida *et al.*, Phys. Rev. Lett. **104**, 100501 (2010).
[13] Yu. I. Bogdanov, arXiv:quant-ph/0312042.
[14] R. Kress, *Numerical Analysis.* (Springer Verlag, New York, 1998).
[15] R. Penrose, Proc. Cambridge Philos. Soc. **51**, 406 (1955).
[16] It holds if one can neglect instrumental uncertainties.
[17] Yu. I. Bogdanov, JETP **108**, 928 (2009).